

# LATTICE SITE OCCUPANCY IN TERNARY ORDERED $\text{Ni}_3\text{Al}_{1-x}\text{Fe}_x$ ALLOYS ESTIMATED BY EXAFS

K. ŁAWNICZAK-JABŁOŃSKA

Institute of Physics, Polish Academy of Sciences  
Al. Lotników 32/46, 02-668 Warszawa, Poland

S. PASCARELLI, F. BOSCHERINI

INFN Laboratori Nazionali di Frascati, CP-13, 00044 Frascati, Rome, Italy

AND R. KOZUBSKI

Institute of Physics, Jagiellonian University, Reymonta 4, 30-059 Kraków, Poland

Extended X-ray absorption fine structure (EXAFS) spectroscopy offers additional experimental evidence to the solution of site occupancy problem in ternary NiAlX alloys. A study of local order in the stoichiometric  $\text{Ni}_3\text{Al}_{1-x}\text{Fe}_x$  ternary alloys ( $x = 0.02, 0.05, 0.10, 0.15,$  and  $0.25$ ) by EXAFS at the *K*-edge of Fe in the energy range from 7000 eV to 7600 eV are presented. Three models of substitutional behavior are considered — the preferential substitution of Fe atoms in: 1) Ni sites, 2) Al sites, 3) both sites. Data analysis was performed with theoretical and experimentally determined scattered photoelectron phases and amplitudes. The results of the EXAFS analysis are consistent with the picture in which most of the Fe atoms substitute Al sites and less than 25% of Fe atoms substitute Ni sites. Alloys with more than 10 at% of Fe showed higher tendency for ordering than those containing less than 10 at% Fe.

PACS numbers: 61.10.Lx, 61.55.Hg

## 1. Introduction

Nickel aluminide  $\text{Ni}_3\text{Al}$  is an intermetallic compound with  $\text{L1}_2$ -type structure and is considered to be a promising high-temperature structural material due to its superior mechanical properties. These properties can be improved by additions of different ternary elements [1]. The influence of these additions can be better understood by determining the distribution of the substitutional elements between the Ni and Al sites of the ordered  $\text{L1}_2$  lattice [2]. The problem of site occupancy on ternary NiAlX alloys is then very important not only for understanding the kinetics

of alloying and order formation but also for prediction of mechanical properties in Ni based superalloys.

Several theoretical and experimental approaches to this problem was reported using different substitutional elements [3–8]. Three types of substitutional behavior in ordered NiAlX alloys can be distinguished, depending on the relative magnitude of Ni–X and Al–X interactions — the preferential substitution of X in: 1) Ni sites, 2) Al sites, 3) both sites.

The present work contributes to a research project aiming to study the  $\text{Ni}_3\text{Al}_{1-x}\text{Fe}_x$  system. Theoretical calculations [3, 4] and some experimental evidences [5–8] suggest that the behavior of Fe does not indicate a strong preference to occupy only Ni or only Al sites; therefore, Fe should be classified as having a substitutional behavior of the third type. Moreover, electron channeling enhanced microanalysis (ALCHEMI) [7] and theoretical considerations [4] indicate that this substitutional behavior of the third type elements is very sensitive to deviations from the stoichiometric composition. It was found that the probability of Fe to substitute Ni sites decreases as the Al content decreases [7]. In fact, in  $\text{Ni}_{70}\text{Al}_{25}\text{Fe}_5$  alloy 72% of Fe atoms substitutes Ni site, but in  $\text{Ni}_{75}\text{Al}_{20}\text{Fe}_5$  this number decreases to 23%.

Extended X-ray absorption fine structure (EXAFS) spectroscopy offers additional experimental evidence to the solution of site occupancy problem. A specific advantage of this technique is the possibility of tuning into an absorption edge of particular element in a compound and thus study of the local bonding properties (bond distance, coordination numbers, and atomic mean square relative displacements) around each element.

We present a study of local order in the stoichiometric  $\text{Ni}_3\text{Al}_{1-x}\text{Fe}_x$  ternary alloys ( $x = 0.02, 0.05, 0.10, \text{ and } 0.15$ ) by EXAFS spectroscopy at the *K*-edge of Fe.

## 2. Experiment and result

The absorption measurements were performed at the PULS synchrotron radiation facility using the emission from the ADONE storage ring of the Laboratori Nazionali at Frascati. The storage ring was operated at 1.2 GeV and the average current was about 60 mA. The spectra were recorded in the fluorescence mode at the Fe *K*-edge in the energy range 7000 eV to 7600 eV. The X-ray radiation was monochromatized using a Si(111) channel-cut crystal. The samples were prepared in a high-frequency furnace under Ar flow and rapidly solidified. In order to form a homogeneous ordered structure all the samples were annealed for one week at temperatures below the order–disorder transition [9]. The homogeneity, effective composition, and microstructures were checked by X-ray diffraction, SEM, and TEM [9]. In the range of standard microanalysis error the composition of all samples was equal to the nominal composition. X-ray diffraction showed the presence of  $L1_2$ -type long-range order in all the alloys and a decrease in lattice parameter from  $a = 3.57 \text{ \AA}$  to  $a = 3.56 \text{ \AA}$  with increasing Fe content  $x$  from 0 to 0.15.

The absorption spectra were analyzed according to standard procedure. The pre-edge region was fitted with a linear function and the absorption above the edge was fitted with two cubic splines to simulate the atomic cross-section.  $E_0$

was chosen at 7113 eV and was treated as an adjustable parameter in the further analysis. The EXAFS oscillations obtained in this way are shown in Fig. 1.

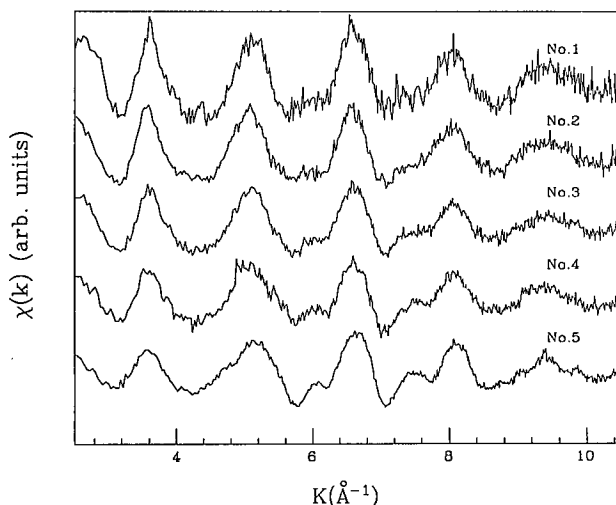


Fig. 1. The raw EXAFS data for  $Ni_{0.75}(Fe_xAl_{1-x})_{0.25}$  after background subtraction. The samples are numbered following increasing Fe content.

The data were multiplied by  $k$  and then Fourier transformed in the range  $k = 2.8-10.5 \text{ \AA}^{-1}$  with a Henning window ( $0.5 \text{ \AA}^{-1}$ ) in order to separate the contribution from the various shells. The Fourier transforms of the  $k\chi(k)$  signal are shown in Fig. 2. They show a typical fcc lattice structure for all samples. At least four coordination shells are seen to contribute to the EXAFS oscillations. It is interesting to note that the first peak, corresponding to the first coordination shell around Fe, is at the same apparent position in all samples, and equal to the position of the first peak in the spectrum relative to metallic Ni. First-shell information was selected by performing a back Fourier transform of the  $R$ -space data in the range  $1.1 < R [\text{\AA}] < 3.2$ .

The structural parameters characterizing the first coordination shell around Fe which can be obtained from an EXAFS analysis are: the number and the type of nearest neighbors (or coordination numbers)  $N_{Fe-Ni}$  and  $N_{Fe-Al}$ , the interatomic distances relative to each bond,  $R_{Fe-Ni}$ ,  $R_{Fe-Al}$  and the values of the mean square relative displacements  $\Delta\sigma^2$  of each bond. These parameters appear in the general EXAFS formula [10] together with the phase shift due to the potential of central atom (Fe) and the phase shift and scattering amplitude relative to the interaction of photoelectron with the neighboring atomic potentials (in principle Ni, Al, and Fe atoms). If these functions are known, the structural parameters can be obtained by performing a least squares fit in which the standard EXAFS formula is used to simulate the first-shell EXAFS oscillations with  $N$ ,  $R$ , and  $\Delta\sigma$  left as free parameters.

Phase shifts and amplitudes are best obtained by measuring EXAFS on

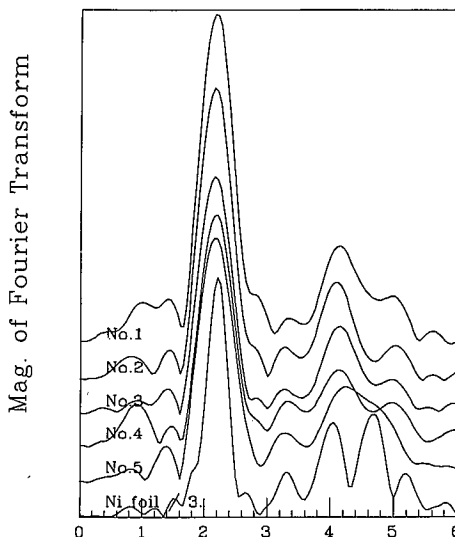


Fig. 2. Fourier transforms of the raw EXAFS signals for  $\text{Ni}_{0.75}(\text{Fe}_x\text{Al}_{1-x})_{0.25}$ . A Henning window in the range  $2.8 \text{ \AA}^{-1}$  to  $10.5 \text{ \AA}^{-1}$  was used.

a model sample in which bonding configurations similar to those investigated are present. The advantages of experimentally determined phase shifts and amplitudes with respect to theoretical values lie in the fact that many-electron effects are left out of the calculations, and as a result the overall amplitude can be difficult to simulate correctly. On the other hand, the experimental determination of the phases and amplitudes relies on their transferability from a known system to an unknown.

The model compounds which reproduce best the bonding configurations present in our alloys are the  $L_{12}$  ordered  $\text{Ni}_3\text{Fe}$  and  $\text{Ni}_3\text{Al}$ . In this structure Ni atoms lie on the face centers, while Fe or Al atoms are situated on the cube corners. At this point we put forward a first hypothesis on the structure of our samples which consists in considering our  $\text{Ni}_3\text{Fe}$  sample to be in an ordered  $L_{12}$  structure. Therefore, the central Fe atom in this sample is bonded to first shell composed of only Ni atoms. The structure of the ternary  $\text{Ni}_3\text{Al}_{1-x}\text{Fe}_x$  alloys then depends on the substitutional behavior of the Fe atoms, which can be of three types:

- a) substitution of only Al sites (corners in the fcc unit cell); each Fe atom has 12 Ni nearest neighbors;
- b) substitution of only Ni atoms (face center in fcc unit cell); each Fe atom has a total of 4 (Al + Fe) nearest neighbors and 8 Ni nearest neighbors;
- c) substitution of both Ni and Al sites; the coordination of Fe atoms is intermediate between case (a) and (b).

Our data analysis procedure was as follows. We started by testing hypothesis (a), in which the central Fe atom is surrounded by only Ni nearest neighbors. The model sample chosen for the Fe-Ni pair was metallic Ni. In this way we

approximate a Fe-Ni interaction with a Ni-Ni interaction. In order to test this approximation, we performed several fits using tabulated phases and amplitudes [10, 11] relative to the two atomic pairs. In particular, the following fitting tests were performed on sample No. 5, in which no Al atoms are present:

1. first shell composed of only Ni atoms (Fe-Ni tabulated values);
2. first shell composed of only Fe atoms (Fe-Fe tabulated values);
3. a central Ni atom with a first shell composed of only Ni atoms (Ni-Ni tabulated values).

The best fits obtained in the three cases were of similar quality, and it was therefore impossible to distinguish the three atomic pairs.

The EXAFS spectrum relative to metallic Ni, measured at  $T = 77$  K, was analyzed using the same procedure described above, and the signal relative to the first coordination shell was filtered and fitted with tabulated phases and amplitudes relative to the Ni-Ni pair. Fitting parameters were the coordination number  $N_{Ni-Ni}$ , the bond distance  $R_{Ni-Ni}$ , the mean square relative displacement  $\Delta\sigma^2_{Ni-Ni}$ , and a damping term  $\exp(-2R\gamma/k)$ -type which simulates the effect of core hole lifetime and mean free path of photoelectron. The values of the best fit parameters are listed in Table I. Since the core hole lifetime damping effect is negligible ( $\Delta t_{core-hole\ lifetime} \sim 0.1\Delta t_{back-scattering}$ ), the photoelectron mean free path  $\lambda$  can be calculated from  $\gamma$ , yielding a value of  $\lambda$  ranging from 8 Å to 16 Å in the energy range 100 eV to 400 eV.

Experimental phases and amplitudes relative to the Ni-Ni pair were then extracted from the filtered EXAFS signal and used in the standard EXAFS formula to obtain the structural parameters relative to the five samples. During the fitting procedure, the coordination numbers  $N_{Fe-Ni}$  and the inelastic damping term  $\gamma$  were found to be strongly correlated. Reliable values for these parameters could not be obtained unless further constraints were added. Two different types of constraints were considered:

- I. The inelastic damping term was set equal to the value found for metallic Ni. This hypothesis was checked by analyzing a model sample of metallic Fe in the same way as done for metallic Ni, and the value of  $\gamma$  obtained was equal to the one found for Ni to within 10%.
- II. The total coordination number in samples was set equal to twelve, which is the value found for metallic Ni, and is common to all fcc structures.

The values of the best fit parameters are listed in Table I and Table II for the two types of constraints, respectively. Note that the quality of the fits, shown in column 8, is similar in the two cases. The filtered EXAFS as well as the best fits for constraint II are shown in Fig. 3.

As can be seen from the two tables, the bond lengths are constant with composition and equal to the expected values in the fcc structure, based on the measured lattice parameters [9].

The most interesting result is the reduction in coordination number with respect to metallic Ni which is evident in all samples, as can be seen from the values listed in Table I. This trend is also visible in Table II, where the total

TABLE I

Values of the structural parameters obtained from the best fits of the first-shell EXAFS signal on assumption that Fe atoms substitute only Al sites and with the constraint that the inelastic damping term  $\gamma$  in the samples has the same value as in metallic Ni. All values relative to samples No. 1–5 are obtained using metallic Ni as a model. The values  $N$  and  $\gamma$  are absolute values while the  $\Delta\sigma^2$  value is relative to the model.

Sample	$x$	$N$	$R_{\text{Fe-Ni}}$ [Å]	$\sigma^2$ [ $\times 10^{-3}$ Å <sup>2</sup> ]	$\gamma$	$\Delta E$ [eV]	Fit $\times 10^{-2}$
1	0.02	8.3	2.49	0.1	0.6	1.0	1.0
2	0.05	7.9	2.49	1.0	0.6	3.0	0.5
3	0.10	8.0	2.49	3.0	0.6	3.0	0.5
4	0.15	6.1	2.50	0.6	0.6	2.0	0.7
5	0.25	6.4	2.49	0.3	0.6	2.0	0.7
Ni foil <sup>a</sup>		12	2.49	4.3	0.6	-12.0	1.0

<sup>a</sup> Theoretical phases and amplitudes used.

TABLE II

Values of the structural parameters obtained from the best fits of the first-shell EXAFS signal on assumption that Fe atoms substitute only Al sites and with the constraint that the total coordination number is equal to twelve. All values relative to samples No. 1–5 are obtained using metallic Ni as a model. The values  $N$  and  $\gamma$  are absolute values while the  $\Delta\sigma^2$  value is relative to the model.

Sample	$x$	$N$	$R_{\text{Fe-Ni}}$ [Å]	$\sigma^2$ [ $\times 10^{-3}$ Å <sup>2</sup> ]	$\gamma$	$\Delta E$ [eV]	Fit $\times 10^{-2}$
1	0.02	12	2.49	1.5	0.9	1.0	1.0
2	0.05	12	2.49	2.6	0.9	3.0	0.5
3	0.10	12	2.49	4.6	0.9	2.0	0.5
4	0.15	12	2.49	3.0	1.1	2.0	0.7
5	0.25	12	2.49	2.4	1.1	2.0	0.7
Ni foil <sup>a</sup>		12	2.49	4.3	0.6	-12.0	1.0

<sup>a</sup> Theoretical phases and amplitudes used.

coordination number was set equal to twelve, as an increase in inelastic damping, due to the strong correlation between  $N$  and  $\gamma$ . On the other hand, the latter results are contradicted by the tests performed on metallic Fe, in which a value of

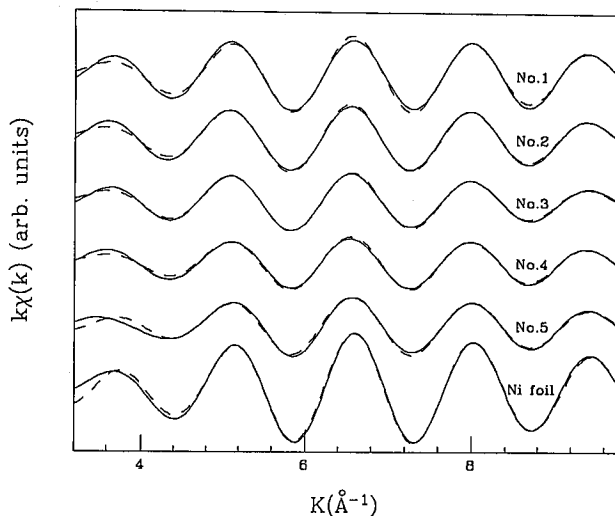


Fig. 3. Best fits to the first-shell EXAFS signal for  $Ni_{0.75}(Fe_xAl_{1-x})_{0.25}$ , obtained on assumption of preferential substitution of Al sites. The EXAFS is shown as the solid line and fits as a dotted line; the EXAFS signal from metallic Ni samples used as a model is also included.

$\gamma$  similar to the one found for Ni was obtained but it can lead also to the conclusion that  $\gamma$  in a system composed of different types of atoms is larger than in a system of one type of atoms.

The analysis procedure continued with the test of hypothesis (b) and (c), in which the central Fe atom is surrounded by all three kinds of atoms. As we have already mentioned, Fe and Ni nearest neighbors cannot be distinguished. We therefore checked on the presence of Al nearest neighbors. Unfortunately, we were not able to find a reliable model sample from the spectrum of which experimental phases and amplitudes can be extracted. Therefore, tabulated values were used for the Fe-Al interaction. The fits performed in the first part of the analysis (in which only Ni(Fe) atoms were included in the first shell) were repeated, and this time a first-shell contribution of Al atoms was added. However, the quality of the fits did not improve.

### 3. Conclusion

The most striking result apparent from the two tables is the decrease in total coordination number or increase in  $\gamma$  parameter in considered alloys. This trend is still not fully understood, and more measurements and analysis are in progress. Anyhow, from the preliminary results of the fitting analysis it seems that there is a tendency of Fe to substitute only Al sites, since the central Fe atom is apparently surrounded only by Ni atoms. On the other hand, the sensitivity of the technique does not allow us to distinguish between Ni and Fe atoms, therefore the presence

of Fe atoms in the first shell cannot be totally excluded. This would lead to a structure in which some Fe atoms lie on the faces of the fcc unit cell. The absence of Al nearest neighbors was tested using tabulated phases and amplitudes, and therefore can be confirmed within the precision of the theoretical data. Taking into account that the limit of the EXAFS sensitivity on coordination number is about  $\pm 10\%$  and that the presence of one Al or Fe atom in the first shell leads to a structure in which 25% of the substitutional Fe atoms enter original Ni sites (face centers in the fcc unit cell), we conclude that this work sets an upper limit to the number of Fe atoms substituting Ni sites, equivalent to the 25% of the total. This result is in agreement with the results of the electron channeling enhance microanalysis [7].

The length of Fe-Ni bond  $R_{\text{Fe-Ni}}$  resulting from our analysis is 2.49 Å and is smaller than 2.52 Å deduced from diffraction measurements [9].

An interesting behavior was observed for the value of the relative mean square displacement  $\Delta\sigma^2$ . This term seems to be inversely proportional to the difference between the concentration of Fe atoms and Al atoms,  $|x_{\text{Fe}} - x_{\text{Al}}|$ , reaching a maximum value when the two concentrations are equal. This is a clear indication of a maximum degree of disorder at  $x_{\text{Fe}} \sim x_{\text{Al}}$ , when the mixed sublattice reaches the maximum number of configurations.

### References

- [1] C.T. Liu, C.L. White, J.A. Horton, *Acta Metall. Mater.* **33**, 213 (1985).
- [2] R.D. Rawling, A. Staton-Bevan, *J. Mater. Sci.* **10**, 505 (1975).
- [3] M. Enomoto, H. Harada, *Metall. Trans. A* **20**, 649 (1989).
- [4] Y.P. Wu, N.C. Tso, J.M. Sanchez, J.K. Tien, *Acta Metall. Mater.* **10**, 2835 (1989).
- [5] M.K. Miller, J.A. Horton, *Scr. Metall. Mater.* **20**, 1125 (1986).
- [6] J.R. Nicholls, R.D. Rawlings, *Acta Metall. Mater.* **25**, 187 (1977).
- [7] D. Shindo, M. Kikuchi, M. Hirabayashi, S. Hanada, O. Izumi, *Trans. Jpn. Inst. Metals* **29**, 956 (1988).
- [8] M. Morinaga, K. Some, T. Kamimura, K. Ohtaka, N. Yukawa, *J. Appl. Crystallogr.* **21**, 41 (1988).
- [9] R. Kozubski, J. Soltys, M.C. Cadeville, V. Oieron-Bohnes, in: *Met. Res. Soc. Symp. Proc.*, Vol. 205, Eds. Thompson, Hviz, Stefanson, Pittsburgh 1992, p. 153.
- [10] B.K. Teo, *EXAFS: Basic Principles and Data Analysis, Inorganic Chemistry Concepts*, Vol. 9, Springer-Verlag, Berlin 1986, p. 26.
- [11] A.G. McKale, B.W. Veal, A.P. Paulikas, S.K. Chan, G.S. Knapp, *J. Am. Chem. Soc.* **110**, 3763 (1988).